Alpha-transfer reactions in light nuclei. III. (^{7}Li, t) stripping reaction*

M. E. Cobern,† D. J. Pisano,‡ and P. D. Parker

Wright Nuclear Structure Laboratory, Yale University, New Haven, Connecticut 06520

(Received 1 March 1976)

The ^{12}C(^{7}Li, t)^{16}O and ^{16}O(^{7}Li, t)^{20}Ne reactions have been studied at a beam energy of 38 MeV. At this energy these reactions exhibit a high selectivity for populating α-particle cluster states. The angular distributions for these states have been analyzed using an exact-finite-range coupled-channels Born-approximation code incorporating final-state cluster wave functions derived from an α-core folded potential. The resulting α-particle spectroscopic factors (S_α) for the 0^+, 2^+, and 4^+ members of the ^{20}Ne ground state band are in good agreement with cluster model predictions. For the 7.12-MeV (1^-) state in ^{16}O, the spectroscopic factor ($S_\alpha \approx 0.20$) is consistent with other analyses but is uncertain by a factor of 2 due to the presence of significant compound-nuclear contributions to this transition. In general, for those states which are not selectively populated at forward angles the measured angular distributions are well described by a Hauser-Feshbach calculation. In particular it is shown that both the magnitude and shape of the angular distributions for the 11.10-MeV (4^+) state populated in the ^{12}C(^{6}Li, d)^{16}O and ^{12}C(^{7}Li, t)^{16}O reactions can be well accounted for in terms of statistical compound-nuclear contributions. The elastic scattering of ^{7}Li ions from several light targets has also been studied and optical-model potentials derived.

[NUCLEAR REACTIONS ^{12}C, ^{16}O, ^{20}Ne(^{7}Li,t), $E(^7\text{Li}) = 38$ MeV, measured $\sigma(E, \theta)$, Hauser-Feshbach and finite-range CCBA analysis, spectroscopic factors.]

I. INTRODUCTION

In the work presented in this series of papers we have examined reactions involving the transfer of four nucleons. The data have been analyzed in terms of a cluster transfer mechanism, and the results have been interpreted in terms of α-particle clusters, as the simplest representation of the summation of the shell model configurations which give rise to the strong, selective population of states which are observed in these reactions. Clearly this interpretation has validity only for those few states which are identified by this selectivity; it is these states which we refer to as "α-cluster" states and which are of primary concern in the work presented in this series of papers.

During the past several years, considerable experimental and theoretical effort has been devoted to the study of α-particle-transfer reactions on p-shell and sd-shell nuclei[1-9] in order to examine the importance of α-particle clustering in this mass region. This information is important for our understanding of the structure of these nuclei and for the analysis of the helium-burning[10, 11] and silicon-burning[12, 13] processes in nuclear astrophysics. In the latter area, by determining the α-particle reduced widths of bound and nearly bound states, α-stripping reactions such as (^{6}Li, d) and (^{7}Li, t) can provide information which is complementary to that obtained from (α, α) elastic scattering and (α, γ) capture reactions and which is essential for the evaluation of the contributions of very low-energy and subthreshold resonances to various nuclear reaction rates at stellar temperatures. Much qualitative information regarding the structure of particular levels has been deduced from these α-stripping reactions, mainly due to their well-documented selectivity. These results have also shown that the (^{7}Li, t) reaction is significantly more selective than the (^{6}Li, d) reaction,[14] suggesting that it is the best candidate for a more quantitative analysis. However, in spite of the pronounced selectivity of the (^{7}Li, t) reaction and the strong forward peaking of the angular distributions, both of which are taken as indications of a direct-transfer reaction mechanism, a quantitative analysis of the results, permitting the extraction of spectroscopic data, has been hampered by several factors:

(1) The relative p state in the α-triton cluster wave function for ^{7}Li precludes the use of the zero-range assumption implicit in "standard" distorted-wave Born-approximation (DWBA) calculations.

(2) Except for a transition between two 0^+ states, this internal motion also necessitates the inclusion of three values for the transferred angular momentum L.

(3) The comparable masses of the three "fundamental" particles in the transfer (α, t, "core") require the inclusion of recoil effects in the evaluation of the transfer matrix element. The first-order recoil corrections sometimes used in the analysis of the transfer of a "light" particle be-

tween two "heavy" cores are not applicable.
(4) There have also been suggestions[15] that multistep processes involving core excitation participate in the reaction, indicating the importance of a coupled-channels analysis.

Previously, various approximations have been used to simplify this problem. Neogy *et al.*[16] employed a plane-wave Born approximation (PWBA) to permit the factorization of the six-dimensional integral in the transfer matrix element. Other authors have used various modifications of the fixed-range or "no-recoil" DWBA formalism.[17,18] A complete, finite-range DWBA treatment, suitable for use in heavy-ion-induced reactions, has been derived by Austern *et al.*[19] and employed in the code LOLA by DeVries.[20] A more complete discussion on these analyses has been presented in Paper I[21] of this series.

In this paper, we report on measurements on the $^{16}O(^7Li, t)^{20}Ne$ and $^{12}C(^7Li, t)^{16}O$ reactions at a beam energy of 38 MeV, and on the analysis of their angular distributions within the framework of the coupled-channels formalism of Ascuitto and Glendenning,[22] with the source term evaluated exactly in finite-range, including recoil, following the Austern method.[19] A description of this code, FRIMP, including the derivation of the relevant formalism, has been presented in Paper I of this series.[21]

II. EXPERIMENTAL PROCEDURE

The experiments were performed at the MP-7 tandem accelerator at Brookhaven National Laboratory. $^7Li^-$ ions were produced using a standard duoplasmatron in conjunction with a lithium-vapor exchange canal[23]; with this combination a beam of 300 to 500 nA of $^7Li^{3+}$ could readily be maintained on target. A gas cell 2.2 cm in diameter with a 0.5-μm nickel entrance foil and a 1.0-μm nickel exit foil was used as the target for the $^{14}N(^7Li, t)^{18}F$, $^{16}O(^7Li, t)^{20}Ne$, and $^{20}Ne(^7Li, t)^{24}Mg$ reactions. Typical gas pressures ranged from ~0.2 to ~0.35 atm. Self-supporting carbon foils with nominal thicknesses of 50 to 100 $\mu g/cm^2$ were used as targets for the $^{12}C(^7Li, t)^{16}O$ reaction.

Triton angular distributions were measured using standard $\Delta E + E$ telescopes of Si(SB) detectors with Radeka pulse multipliers[24] used for particle identification. The total resolution for the system was typically 120–180 keV. Peak areas were extracted using a fitting program which incorporated a polynomial background for the low-energy triton continuum and which could analyze unresolved multiplets in terms of sum of Gaussians whose relative widths could be externally restricted on the basis of kinematics considerations, etc.

III. RESULTS

A typical forward-angle spectrum obtained for the $^{12}C(^7Li, t)^{16}O$ reaction at 38-MeV incident energy, shown in Fig. 1, displays the extreme selectivity of this reaction. The spectrum is dominated by the members of the 4p-4h, $K^\pi = 0^+$ band [6.05 MeV (0^+), 6.92 MeV (2^+), 10.35 MeV(4^+), and 16.30 MeV (6^+)] and the $K^\pi = 0^-$ α-cluster band[9]

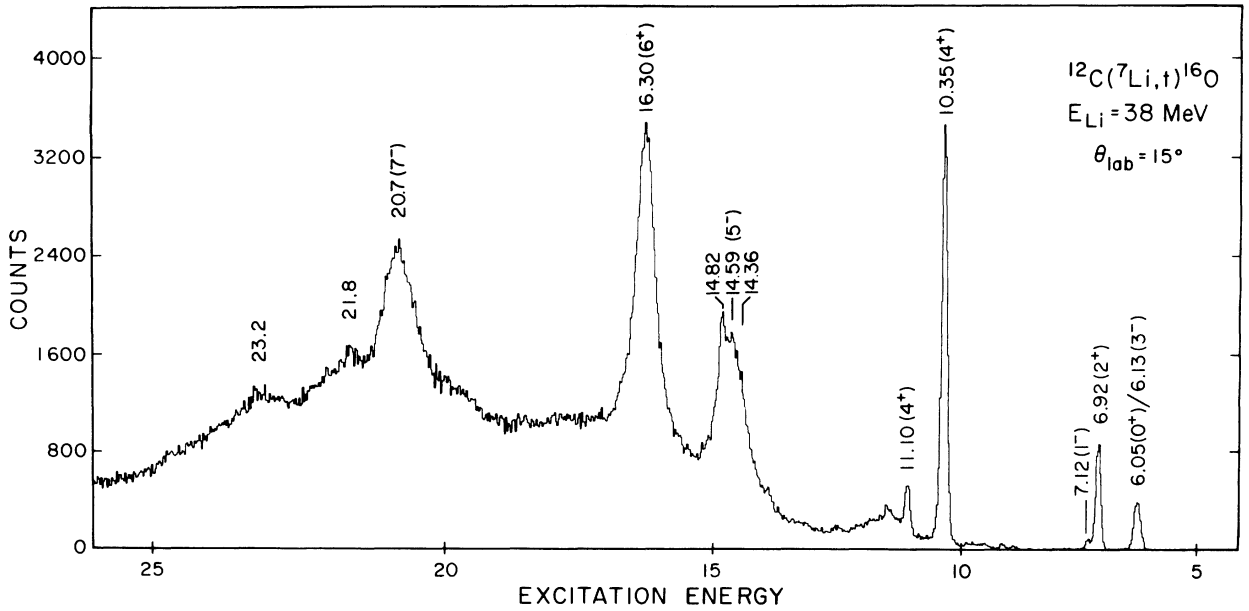

FIG. 1. Triton energy spectrum measured at $\theta_{lab} = 15°$ for the $^{12}C(^7Li, t)^{16}O$ reaction at a bombarding energy of 38 MeV. At this angle the spectrum is dominated by direct transitions to states such as the members of $K^\pi = 0^+$ and 0^- bands which have large widths for ($^{12}C + \alpha$) clustering.

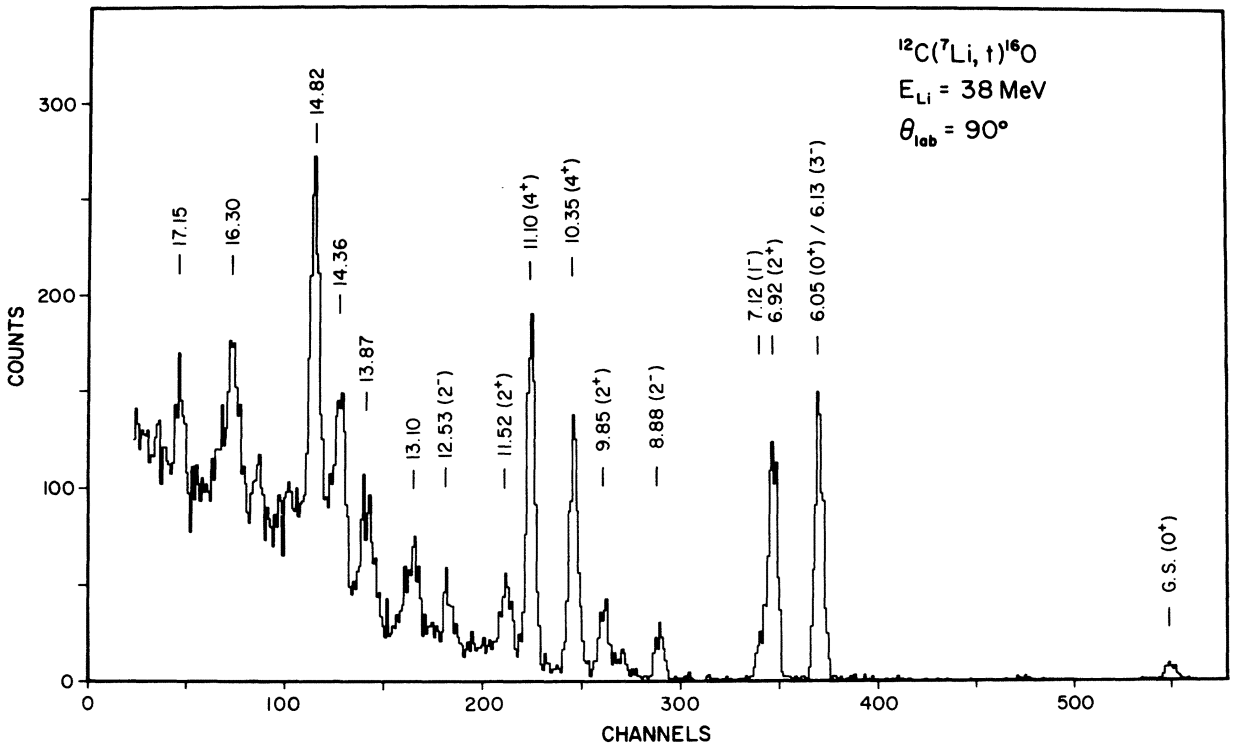

FIG. 2. Triton energy spectrum measured at $\theta_{lab} = 90°$ for the $^{12}C(^7Li,t)^{16}O$ reaction at a bombarding energy of 38 MeV. In comparison with Fig. 1, at this angle the spectrum is much more characteristic of a statistical, compound-nuclear model for the reaction mechanism.

[9.60 MeV (1^-), 11.63 MeV (3^-), 14.59 MeV (5^-),[25] and 20.7 MeV (7^-)[25]]. The next members of these bands, $J^\pi = 8^+$ and 9^-, respectively, might be expected at $E_x \approx 26$ to 30 MeV. The selectivity shown in Fig. 1 disappears at more backward angles, e.g., Fig. 2 at $\theta_{lab} = 90^0$, where the general population of states (including those of unnatural parity) is much more characteristic of a statistical, compound-nucleus reaction mechanism. In fact, as discussed below in Sec. V, the angular distributions for those states which are only weakly populated at forward angles are generally well fitted by a Hauser-Feshbach statistical model calculation.

Figure 3 shows a typical forward-angle triton spectrum from the $^{16}O(^7Li, t)^{20}Ne$ reaction. Of the more than 50 known levels with excitation energies below 12 MeV, the only states populated with any appreciable strength are the members of the $K^\pi = 0^+$ ground-state band [0.00 MeV (0^+), 1.63 MeV (2^+), 4.25 MeV (4^+), and 8.78 MeV (6^+)] and the $K^\pi = 0^-$ band [5.79 MeV (1^-), 7.17 MeV (3^-), 10.26 MeV (5^-), and 15.34 MeV (7^-)]. There is no evidence in this spectrum for the significant population of any of the other well established[26] rotational bands in ^{20}Ne. The 8^+ level at 11.95 MeV, thought to be a member of the ground-state band, is singularly absent, barely discernible at the most forward angles and indistinguishable from the background at others. The weak population of this state can be understood in terms of its small reduced α width,[27] but it is also interesting to note that the folded-potential model of Vary and Dover[28] predicts that this state should be found at considerably higher excitation energy, perhaps as high as 15 MeV which would also be more consistent with the simple $J(J+1)$ energy dependence.[29] The next member (9^-) of the $K^\pi = 0^-$ band is predicted by a simple $J(J+1)$ expansion to lie in the region 22 MeV $\lesssim E_x \lesssim$ 24 MeV. In the 10-MeV region from 12 to 22 MeV there are seven states (excluding the 15.34-MeV level) which are highly selectively populated by the (^{7}Li, t) reaction, but whose characteristics are almost completely unknown.

As a part of the same series of experiments, the reactions $^{14}N(^7Li, t)^{18}F$ and $^{20}Ne(^7Li, t)^{24}Mg$ were also investigated. The ^{18}F data are described elsewhere[30]; a typical forward-angle spectrum for the $^{20}Ne(^7Li, t)^{24}Mg$ reaction is shown in Fig. 4. Although this reaction is apparently not as highly selective as the $^{12}C(^7Li, t)^{16}O$ and $^{16}O(^7Li, t)^{20}Ne$ cases [probably due to the $(sd)^4$ configuration of the ^{20}Ne ground state whose valence nucleons can

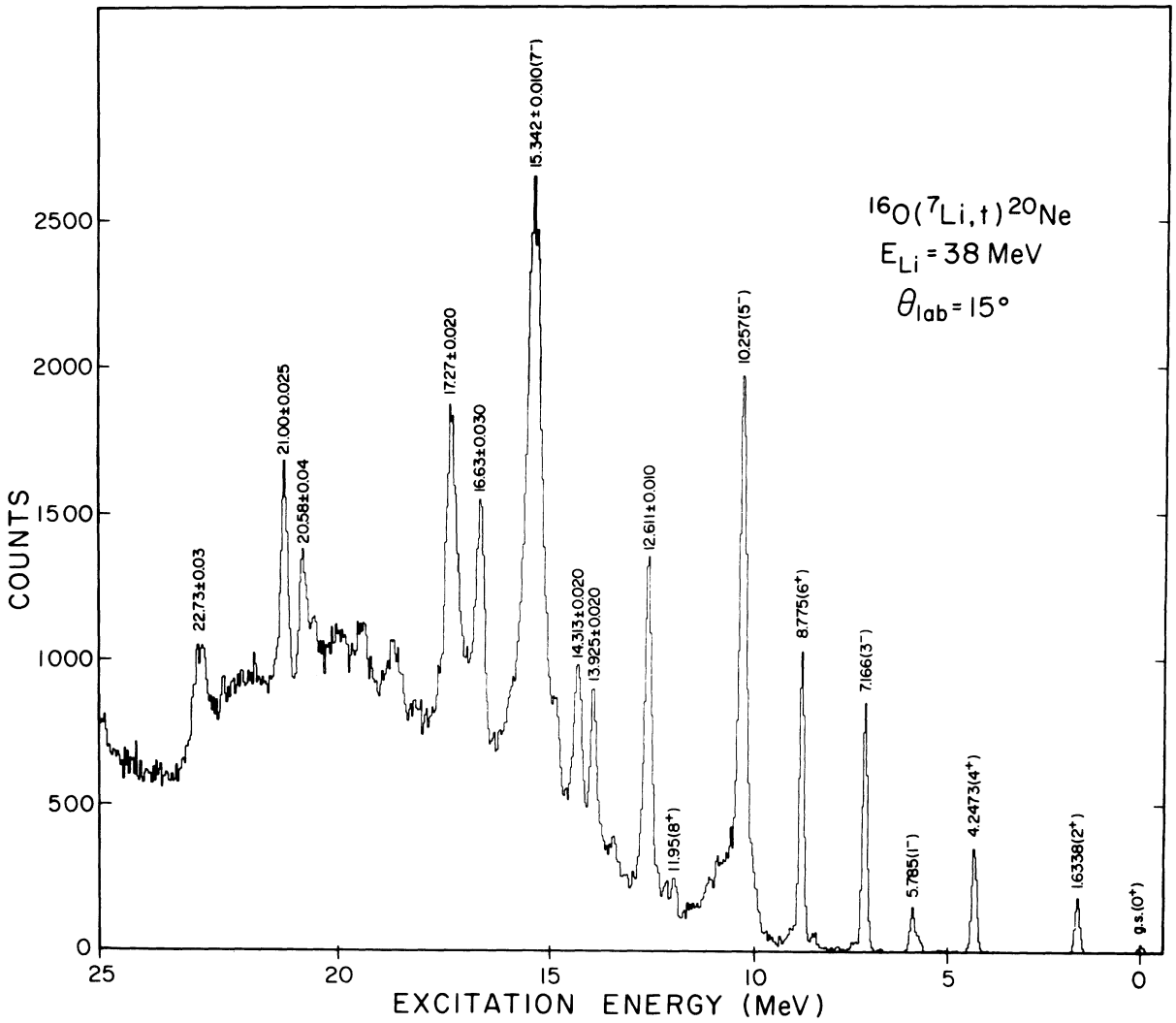

FIG. 3. Triton energy spectrum measured at $\theta_{lab} = 15°$ for the $^{16}O(^{7}Li,t)^{20}Ne$ reaction at a bombarding energy of 38 MeV. As in the case of the 15° spectrum for the $^{12}C(^{7}Li,t)^{16}O$ reaction in Fig. 1, at this angle the spectrum is dominated by direct transitions to states such as the members of the $K^{\pi} = 0^{+}$ and 0^{-} bands which have large widths for $(^{16}O + \alpha)$ clustering.

be coupled to the transferred particles in a greater variety of ways than is possible for the ^{12}C and ^{16}O targets], it still strongly populates only a few states per MeV while the level density is 10 to 100 times larger. It is interesting to note that below an excitation energy of 12.5 MeV the most strongly populated states are the $K^{\pi} = 0^{-}$ band members[31] [7.55 MeV (1^{-}), 8.36 MeV (3^{-}), 10.03 MeV (5^{-}), and 12.42 MeV (7^{-})]. At higher excitation energies, the selectivity is similar to, but not identical to, the selectivity of the $^{12}C(^{16}O,\alpha)^{24}Mg$ reaction. In contrast, however, to the $^{12}C(^{16}O,\alpha)^{24}Mg$ case where the selectively populated states undergo rapid fluctuations as a function of the incident beam energy,[32] in the case of the $^{20}Ne(^{7}Li,t)^{24}Mg$ reaction, there are apparently no rapid fluctuations with bombarding energy since spectra measured at 30 MeV[33] and at 36 and 38 MeV (with beam energy resolutions of $\Delta E_{c.m.} \approx 120$ keV) all show a very similar selective population of the same states, indicative of the direct nature of the $(^{7}Li, t)$ reaction populating these levels.

Further evidence of a relatively strong direct component in the $(^{7}Li, t)$ reaction mechanism can be seen in the nature of the states which are selectively populated at forward angles. It is clearly not just a selection of high-spin states on the basis of angular momentum matching; there are many more states with high spin [e.g., the 8.45-MeV (5^{-}) 5p-1h) and 12.15-MeV (6^{+}) (8p-4h) states in ^{20}Ne] which are notably absent. Instead, the strong selectivity seen in the forward-angle spec-

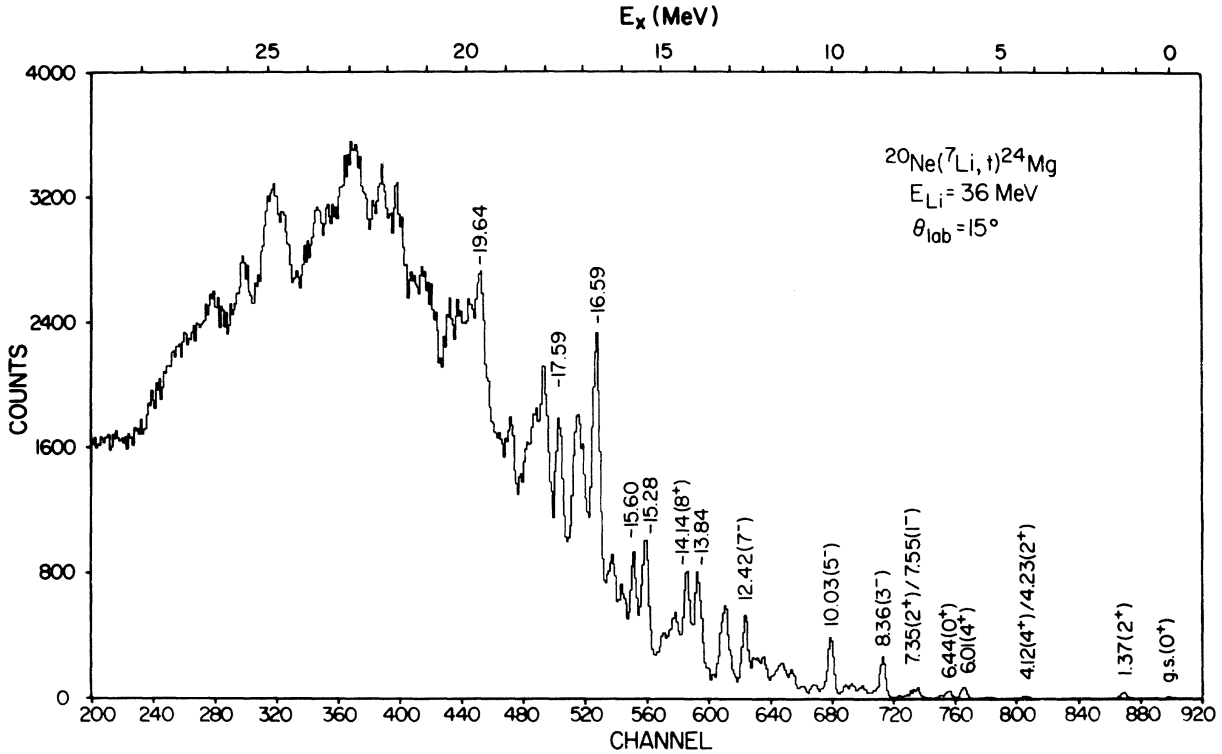

FIG. 4. Triton energy spectrum measured at $\theta_{lab} = 15°$ for the ^{20}Ne(^{7}Li,t)^{24}Mg reaction at a bombarding energy of 36 MeV. For $E_x < 12.5$ MeV the strongest states in the spectrum are the members of the $K^\pi = 0^-$ band starting with the 7.55-MeV (1^-) state.

tra is related to the *structure* of the states, with strong transitions to the $K^\pi = 0^+$ and 0^- α-cluster rotational bands and with much weaker transitions to those states with small α-particle reduced widths, such as the ^{16}O levels at 8.87 MeV (2^-), 9.85 MeV (2^+), 11.10 MeV (4^+) and the ^{20}Ne levels at 4.97 MeV (2^-), 8.45 MeV (5^-), 12.15 MeV (6^+), etc. This indication of the relative unimportance of nondirect components in the (^{7}Li, t) transitions to the strongly populated states supports the validity of a direct-reaction analysis of their angular distributions. [In the case of the (^{6}Li, d) reaction, such faith is not as clearly justified because more substantial nondirect contributions are evident in the forward angle spectra.[15, 34]]

The analysis of the ^{12}C(^{7}Li, t)^{16}O and ^{16}O(^{7}Li, t)^{20}Ne angular distributions is described below in Secs. V and VI.

IV. ELASTIC SCATTERING–OPTICAL MODEL ANALYSIS

In order to determine optical model parameters for the elastic scattering of ^{7}Li ions in this energy range, we have studied the elastic and inelastic scattering angular distributions for ^{12}C, ^{14}N and ^{20}Ne targets (see Fig. 5). The measured angular distributions were analyzed using the optical mo-

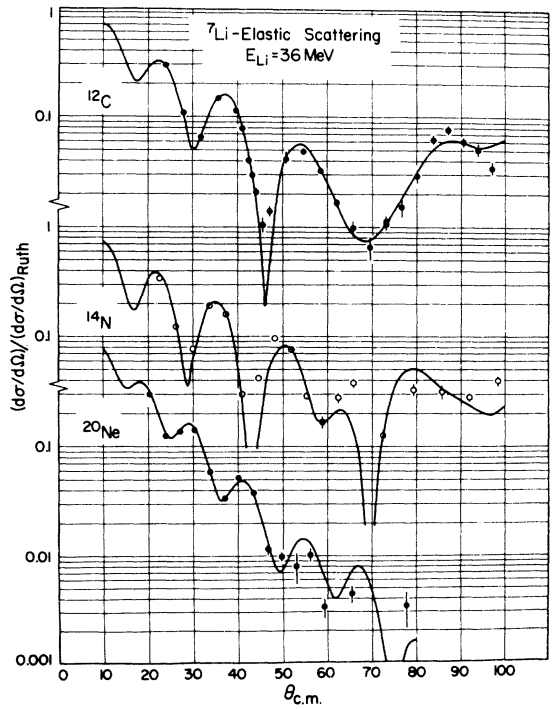

FIG. 5. Angular distributions measured for ^{7}Li elastic scattering on ^{12}C, ^{14}N, and ^{20}Ne. The curves are optical model fits to the data using the parameters listed in Table I.

TABLE I. Optical model parameters for lithium-7 scattering at 36 MeV:

$$U(r) = V_C - Vf(x) + 4iW_D \frac{d}{dr} f(x_I) ,$$

where

$$V_C = Z_1 Z_2 e^2 \begin{cases} 1/r, & r > R_C \\ \left(3 - \frac{r^2}{R_C^2}\right)/2R_C, & r \leq R_C \end{cases} , \quad R_C = r_{0C} A^{1/3} ,$$

$$f(x) = (1+e^x)^{-1}; \quad x = \frac{r - r_0 A^{1/3}}{a} .$$

Target	V (MeV)	r_0 (fm)	a (fm)	W_D (MeV)	r_{0I} (fm)	a_I (fm)	r_{0C} (fm)
^{12}C	160	1.086	0.829	8.710	1.550	1.056	2.50
^{14}N	160	1.031	0.906	12.747	1.754	0.685	2.24
^{20}Ne	197.5	1.009	0.878	22.517	1.448	0.822	2.13
"^{16}O"	160	1.02	0.9	16	1.6	0.8	2.2

del parameter search code JIB3 [35] The starting values for the real well depth and radius were systematically varied over a large region to investigate the behavior of different "families" of continuously ambiguous parameters (cf. Ref. 36). In contrast to previous studies at lower beam energies, [37, 38] our best fits were obtained with well depths in the range of 160–200 MeV. The back-angle data $\theta_{c.m.} \gtrsim 90^0$ were the most critical in differentiating between the various possible parameter sets. The "best-fit" parameters are listed in Table I, together with an average potential for the ^{7}Li + ^{16}O system derived from the others by interpolation. The calculated curves for these potentials are shown in Fig. 5.

Our measured cross sections are in good agreement where they overlap with the recent results of Schumacher *et al.*[39]. While our derived (real) potential is somewhat shallower than, but otherwise quite similar to, the "Family III" potentials of Ref. 39, it should be noted that the region $\theta_{c.m.} \gtrsim 90^0$, which we found to be the most crucial in choosing between parameter sets, was not included in the measurements and analysis of Schumacher *et al.*

V. HAUSER-FESHBACH ANALYSIS

While there is strong experimental evidence that many transitions in the (^{7}Li, t) reaction are primarily direct in nature, many other transitions, such as those which are observed to non-natural parity states, cannot take place via a simple one-step direct α-transfer reaction. Statistical compound-nuclear effects should be important for such cases and may also be significant at back angles even for those cases which look like direct reactions at forward angles.

In order to determine the magnitude of these compound-nuclear effects, a Hauser-Feshbach (HF) calculation was performed using the code STATIS.[40] This code differs from simpler statistical compound-nuclear programs in two important respects:

(1) Up to six fragmentations of the compound nucleus can be included in the calculation, so that all of the significant open channels may be treated explicitly.

(2) The energies and spins of the known levels of the compound system and of each heavy fragment can be specified, with the statistical formula for the level density employed only in the energy region beyond the highest measured state.

These modifications remove two of the chief sources of uncertainty in the magnitude of such HF curves. Using this code, experimental compound-nuclear cross sections for several different heavy-ion-induced reactions have been reproduced to within a factor of 2, without any renormalization.[41] In the present analyses the n, p, d, t, α, and ^{7}Li channels were included in the calculation. The level density parameters[42] and optical model potentials[43, 44] for each of these channels were taken from the literature (except for the ^{7}Li potentials which were determined in the present work) with no attempts at parameter variation in order to improve the agreement between the calculations and the measured data. The details of the calculation are given in Ref. 45.

For the ^{12}C(^{7}Li, t)^{16}O reaction the overall magnitude of the HF calculation was determined by normalizing to the measured angular distribution for the 8.87-MeV 2^- level. With this normalization (a factor of 0.125), the calculation reproduces quite well the measured angular distribu-

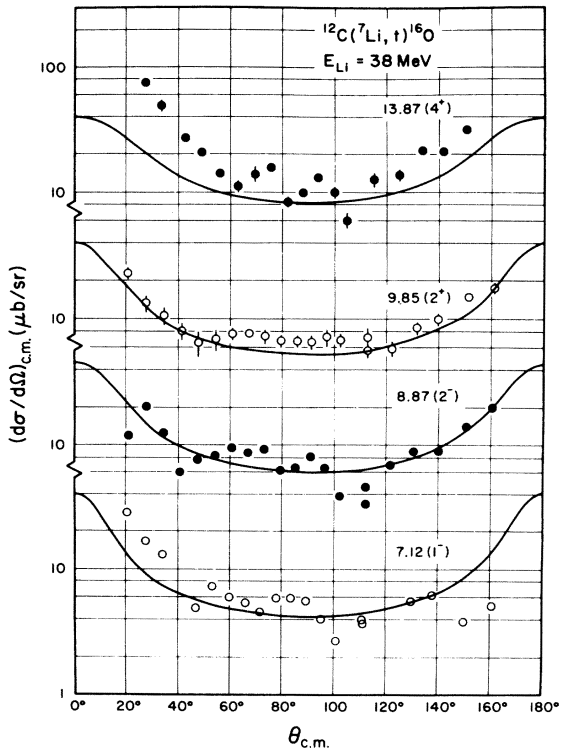

FIG. 6. $^{12}C(^7Li,t)^{16}O$ angular distributions. The curves are predictions of a Hauser-Feshbach calculation whose overall normalization was determined by fitting to the measured angular distribution for the 8.87-MeV (2^-) state.

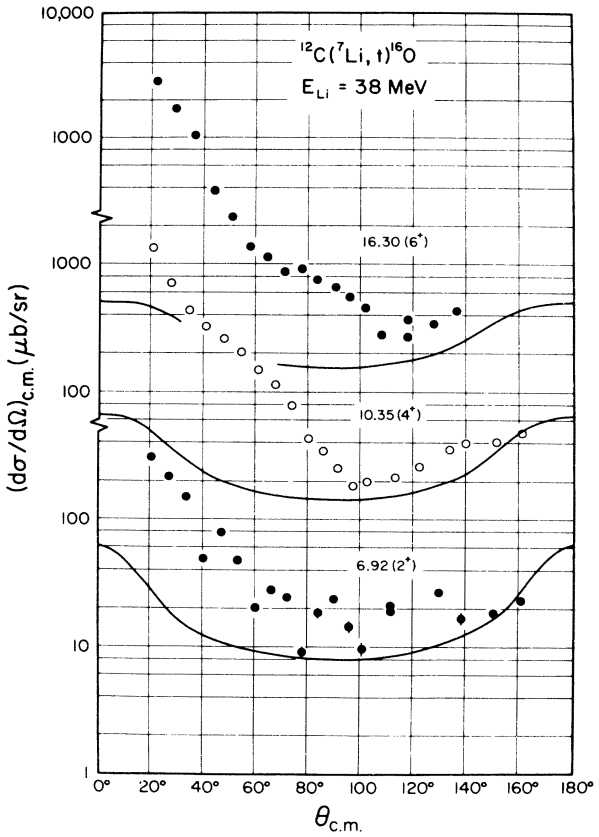

FIG. 7. $^{12}C(^7Li,t)^{16}O$ angular distributions for transitions to the 2^+, 4^+, and 6^+ members of the $K^\pi = 0^+$, 4p-4h band. The curves are the predictions of a Hauser-Feshbach calculation whose overall normalization was determined by fitting to the measured angular distribution for the 8.87-MeV (2^-) state.

tions for the other weakly populated states (e.g., Fig. 6) and can also account for the back-angle cross sections for those states which are more strongly populated at forward angles, e.g., Figs. 7–9. The transitions to the members of $K^\pi = 0^+$ and 0^- bands clearly have important direct components, as seen in the strong forward peaking of their angular distributions in Figs. 7 and 8. Although accurate angular distributions could not be extracted for the 9.60 (1^-) and 11.63 (3^-) members of the 0^- band, it is clear from a comparison of the 15° and 90° spectra in Figs. 1 and 2 that their angular distributions are similar to those for the other 0^- band members and are much more strongly forward peaked than the angular distributions for states such as the 8.87 (2^-), 9.85 (2^+), 11.10 (4^+), etc.

The generally good agreement between the HF calculation and the back-angle data for all of the other transitions plotted in Figs. 6–9 suggests that the spin of the 14.36-MeV state is 6^+ or at least 5^-. The best determination of the energy of the "14.36-MeV" state in our data comes from a comparison with the 6^+ state at 14.815 MeV and yields an excitation energy of 14.363 ± 0.015 MeV. This is apparently not the 4^+ state reported at 14.39 ± .025 MeV[46] and not the 5^+ state seen at 14.400 ± 0.003 MeV in the $^{14}N(\alpha, d)\,^{16}O$ reaction.[47] Although it is easy to understand the strong, direct contributions in the transitions to the $K^\pi = 0^+$ and 0^- bands, it is not clear how to interpret the forward peaking of the $E_x = 14.36$ and 14.82 MeV angular distributions, especially since the 14.82-MeV state is described as having a very pure 2p-2h configuration.[47, 48]

In view of the small reduced width for α decay from the 11.10-MeV 4^+ state in ^{16}O to the ground state of ^{12}C $[\theta_\alpha^2(11.10)/\theta_\alpha^2(10.35) \approx 0.004]$ the relatively strong population of this state observed at forward angles in the $^{12}C(^6Li, d)\,^{16}O$ reaction [at $\theta_{c.m.} \approx 10^0$, $(d\sigma/d\Omega)_{11.08+11.10}/(d\sigma/d\Omega)_{10.35} \sim \frac{1}{2}$] has been cited[15] as evidence for the importance in this reaction of two-step processes involving elastic excitation of the ^{12}C core to its 4.44-MeV 2^+ level, consistent with a $^{20}Ne(2^+) \otimes {}^{12}C(2^+)$ configuration for the 11.10-MeV state. In the $^{12}C(^7Li, t)^{16}O$ reaction, the 11.08 +11.10 MeV states are not popu-

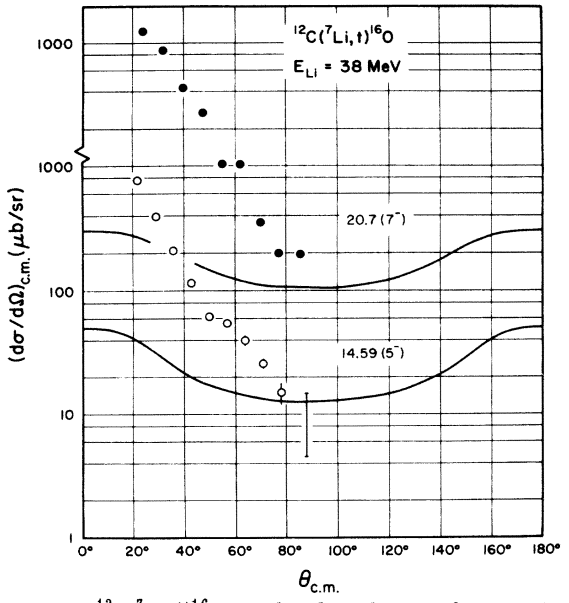

FIG. 8. $^{12}C(^7Li,t)^{16}O$ angular distributions for transitions to the 5^- and 7^- members of the $K^\pi = 0^-$ band based on the 9.60-MeV (1^-) state. The curves are predictions of a Hauser-Feshbach calculation whose overall normalization was determined by fitting to the measured angular distribution for the 8.87-MeV (2^-) state.

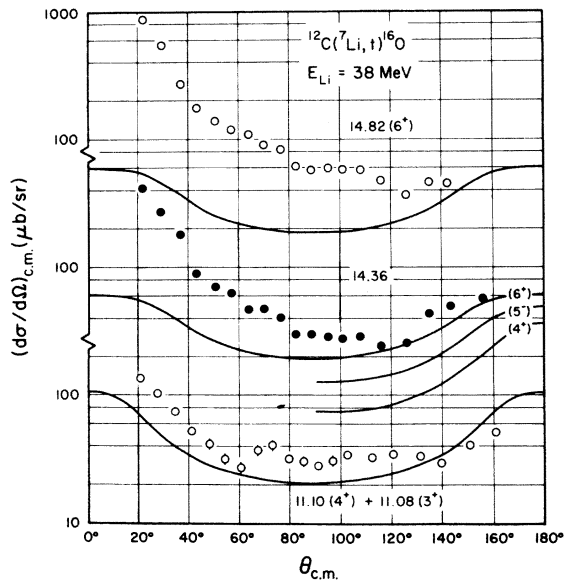

FIG. 9. $^{12}C(^7Li,t)^{16}O$ angular distributions. The curves are predictions of a Hauser-Feshbach calculation whose overall normalization was determined by fitting to the measured angular distribution for the 8.87-MeV (2^-) state. The curve for the 11.1-MeV doublet is the sum of the predicted angular distributions for the 3^+ state and the 4^+ state. (Any additional contribution due to the nearby 0^- state at 10.95 MeV amounts to only a few percent correction to this curve.) The significance of the three curves for the 14.36-MeV state is discussed in the text.

lated nearly so strongly relative to the 10.35-MeV state. A comparison of the angular distributions for these two reactions [Figs. 7 and 9 for $^{12}C(^7Li, t)^{16}O$ and Fig. 10 for $^{12}C(^6Li, d)^{16}O$] shows that compound-nuclear contributions [normalized to the 8.87-MeV (2^-) state] are much stronger in the ($^6Li, d$) reaction [$(d\sigma/d\Omega)_{HF}$ ($^6Li, d$) ~ $5(d\sigma/d\Omega)_{HF}$ - ($^7Li, t$)]. The relatively strong population of the 11.08/11.10 MeV states in the $^{12}C(^6Li, d)^{16}O$ reaction can apparently be understood simply in terms of the strong compound-nuclear contributions to this reaction. Although the direct and compound-nuclear contributions cannot be separated by simple subtraction from the measured cross sections,[49] the greater relative importance of the compound-nucleus reaction mechanism in the ($^6Li, d$) case is evident from the fact that the Hauser-Feshbach calculation is $\gtrsim \frac{1}{2}$ the measured ($^6Li, d$) cross section to the 10.35-MeV state and can account for essentially all of the measured cross sections to the 11.08/11.10 MeV states, whereas the forward-angle cross section for the $^{12}C(^7Li, t)^{16}O$ transition to the 10.35-MeV state is ≈ 30 times larger than the calculated compound-nuclear cross section. This again emphasizes the advantages of ($^7Li, t$) over ($^6Li, d$) as a direct reaction and indicates the danger in drawing any conclusions about second-order direct processes from the ($^6Li, d$) transi-

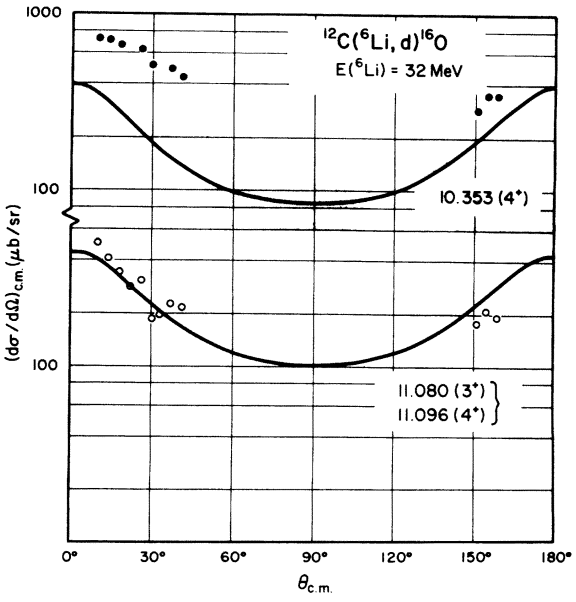

FIG. 10. $^{12}C(^6Li, d)^{16}O$ angular distributions. The data are taken from Ref. 15. The curves are the predictions of a Hauser-Feshbach calculation whose overall normalization was determined by fitting to the 8.87-MeV (2^-) cross section at $\theta_{lab} = 8°$ as measured in Ref. 15. A comparison between these ($^6Li, d$) results and the ($^7Li, t$) results in Figs. 7 and 9 is discussed in the text.

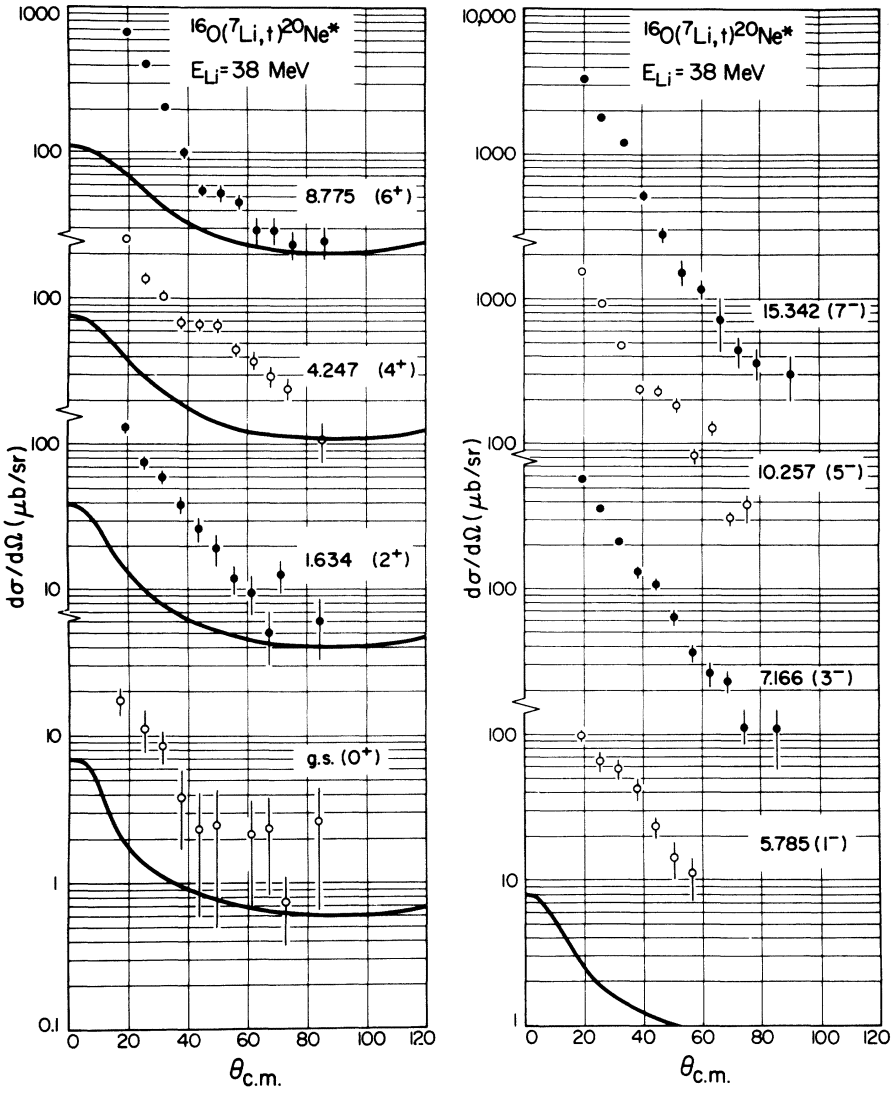

FIG. 11. $^{16}O(^7Li,t)^{20}Ne$ angular distributions to the members of the lowest $K^\pi = 0^+$ and $K^\pi = 0^-$ bands. The curves are the predictions of a Hauser-Feshbach calculation whose overall normalization was determined by fitting to the measured angular distribution for the 4.97-MeV (2^-) state. For the $K^\pi = 0^-$ band the Hauser-Feshbach calculation grossly underestimates the measured cross sections (as discussed in the text); therefore, in order to avoid confusion in this figure only the prediction for the 5.79-MeV (1^-) state is shown.

tions to these two 4^+ states.

For the $^{16}O(^7Li, t)^{20}Ne$ reaction, the Hauser-Feshbach calculation was normalized (a factor of 0.14) by matching the calculation to the measured angular distribution for the 4.97-MeV (2^-) state. Since the $^{16}O(^7Li, t)^{20}Ne$ angular distributions were not measured at center-of-mass angles beyond 90° we cannot make as clear a comparison between the HF calculation and the data for the $^{16}O(^7Li, t)^{20}Ne$ transitions with strong direct components (e.g., Fig. 11) as we could in the $^{12}C(^7Li, t)^{16}O$ case. For the $K^\pi = 0^+$ band, it is clear that the calculated angular distributions are quite consistent with the data. For the $K^\pi = 0^-$ band, the calculated angular distributions underestimate the measured cross sections by a factor of ≈ 5 at $\theta_{c.m.} \approx 80°$ and by nearly a factor of 100 at 20°. In order to avoid confusion in Fig. 11, only the (1^-) curve has been plotted; its magnitude relative to the measured (1^-) angular distribution is typical of the results for the other members of this band. The very strong direct component in the reaction mechanism populating these states dominates these transitions even at $\theta_{c.m.} \approx 90°$. With regard to the discussion in Sec. III, it should also be noted here that this Hauser-Feshbach calculation is in

good agreement with the measured shape and magnitude of the 11.95-MeV (8^+) angular distribution.

VI. FINITE-RANGE DWBA AND COUPLED-CHANNELS BORN-APPROXIMATION ANALYSES

As described in Sec. I, "conventional" DWBA codes, using zero-range or "no-recoil" approximations are inadequate to analyze the results of (^{7}Li, t) reactions. We have therefore used the source term, coupled-equation method of Ascuitto and Glendenning[22] with the source term calculated in the first-order Born approximation in an exact-finite-range framework including recoil.[19] Since the details of the calculation have been given elsewhere,[21, 45] they will not be repeated here. In all of the calculations that follow, a post approximation was used, and the stripping interaction was taken to be simply $V(t - {}^4\text{He})$, the potential that binds the triton and α clusters in the ^{7}Li nucleus. The validity of omitting the Coulomb terms from the interaction potential was checked by carrying out a calculation for the ^{12}C(^{7}Li, t)^{16}O reaction in which the full set of Coulomb terms was included. A comparison between the results of this calculation and one in which the Coulomb terms were not included showed that the two calculations produced angular distributions with nearly identical shapes and with only a 3% difference in absolute magnitude. This is consistent with the results reported earlier by DeVries[20] in a study of stripping interactions for multinucleon-transfer calculations.

A. ^{20}Ne ground-state band

In the analysis of the ^{16}O(^{7}Li, t)^{20}Ne data, several simplifications can be made. The 6-MeV gap between the ground and lowest excited states in ^{16}O strongly inhibits the excitation of these levels by the inelastic scattering of the ^{7}Li ions and suggests that we can neglect inelastic effects in the entrance channel. This assumption is supported by the complete absence (beyond small contributions that can be ascribed to compound-nuclear effects) of the population of any states in ^{20}Ne, such as the members of the well known ^{20}Ne 5p-1h and 8p-4h bands, which could be populated via two-step processes involving 1p-1h and 4p-4h inelastic excitations, respectively, in the ^{16}O core. We can also conclude from the absence of such states that particle-hole core excitations in the exit channel are negligible, so that we are justified in considering only collective effects in a coupled-channels analysis of the exit channel, including the first three members of the ground-state rotational band.

The interaction causing these collective excitations in the exit channel can be described by a deformed optical potential, expanded in spherical harmonics with (static) deformations as coefficients. This technique has been successfully applied by Glendenning[50] to inelastic α scattering from deformed nuclei. In the present analysis we adopted the values[51] $\beta_2 = +0.47$ and $\beta_4 = +0.28$. The wave functions for the bound states of ^{20}Ne were derived from an α-core folding potential by Vary and Dover.[28] Using this potential, these authors were able to reproduce, not only the energies of the

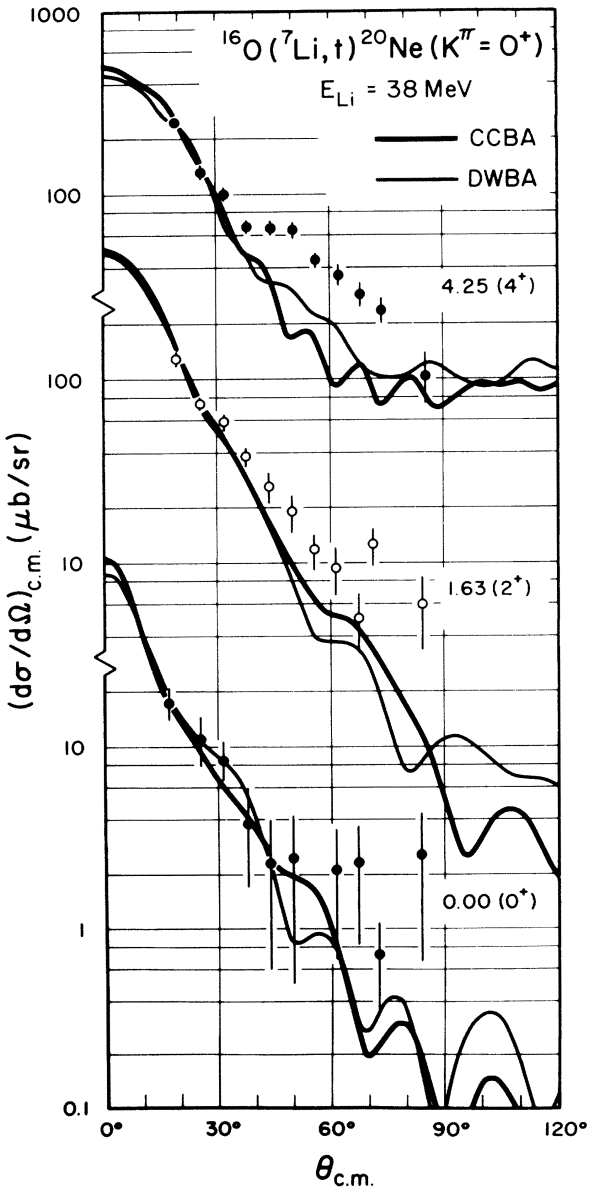

FIG. 12. Exact-finite-range DWBA and CCBA analyses of the ^{16}O(^{7}Li,t)^{20}Ne ($K^\pi = 0^+$) data. The significance of the normalization of the curves is discussed in the text. The extracted spectroscopic factors are presented in Table II.

relevant states in ^{20}Ne, but the widths and transition rates as well, in spite of the fact that the potential has only one free parameter, corresponding to the depth of the central potential. For the ^{7}Li nucleus, an harmonic oscillator wave function (adjusted to give the measured rms radius) was employed. Both wave functions were matched to exponential tails in the extranuclear region ($R \gtrsim 6$ fm). The stripping potential was taken to be a Woods-Saxon well that gives the correct α-t binding energy and radius.[18] The ^{7}Li-^{16}O optical potential listed in Table I was employed for the entrance system; a general triton-nucleus potential, derived by Garrett and Hansen for an analysis of (t,p) reactions on s-d shell nuclei, was used in the exit channel (recipe I of Ref. 44).

Ascuitto and Glendenning have shown that the coupled-channels Born-approximation (CCBA) calculation reduces to the DWBA when the coupling between the intermediate state vanishes.[22] Thus, by "turning off" the collective interaction (i.e., setting $\beta_2 = \beta_4 = 0$) in the CCBA code FRIMP,[21] we can reproduce an exact-finite-range DWBA calculation. Such calculations for the 0^+, 2^+, and 4^+ members of the ground-state rotational band are shown in Fig. 12 together with the CCBA curves. In these transitions the inclusion of the two-step contributions does not significantly change the shapes of the calculated angular distributions because the simple, one-step process is allowed and has a reasonably large spectroscopic factor so that its contribution dominates the CCBA calculation. This is clearly shown in Fig. 13 which compares the contributions for the various one- and two-step processes included in the present analysis for the ^{16}O(^{7}Li, t)^{20}Ne(1.63-MeV; 2^+) transition. This situation is in sharp contrast to the ^{24}Mg(^{3}He, ^{7}Be)^{20}Ne transition to this same state which was discussed in Papers I and II of this series; in that case the small overlap of the initial and final states greatly enhances the relative importance of the second-order processes so that many of the two-step contributions are larger than the simple, one-step contribution. Similar contrasts between "simple, one-step" and "complex, multistep" transitions have been noted for single-nucleon-transfer reactions.[52]

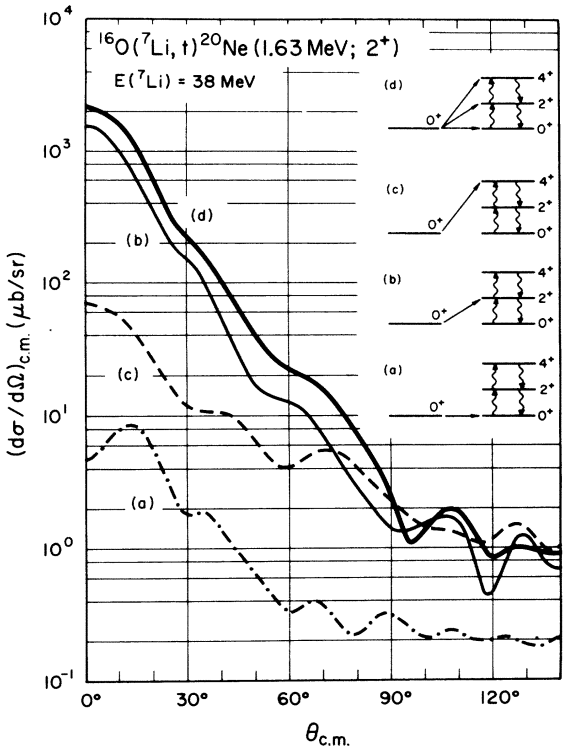

FIG. 13. Comparison of the components in the CCBA analysis of the ^{16}O(^{7}Li,t)^{20}Ne(1.63-MeV, 2^+) transition. Curve (d) is the same as the 1.63 (2^+) CCBA curve in Fig. 12. Although the normal one-step transition is the dominant contribution in this case the two-step transitions through the 0^+ and 4^+ states do make significant contributions to the magnitude of the calculation and the extracted spectroscopic factors in Table II.

Although the two-step contributions are relatively small in the present case they can have important effects in the magnitude of the calculated cross sections, e.g., Fig. 13, because of the interference between these processes. In the calculation of the finite-range DWBA cross sections, both the ^{7}Li and ^{20}Ne wave functions were normalized to unity. Therefore, the normalization of the calculations to the measured cross section determines the pro-

TABLE II. Relative α-cluster spectroscopic factors in ^{20}Ne. (When available, the absolute spectroscopic factor for the ground state is listed in parentheses.)

E_x, J^π	(^{7}Li,t) 38 MeV FRDWBA (Present experiment)	(^{7}Li,t) 38 MeV FRCCBA (Present experiment)	(^{6}Li,d) 32 MeV LOLA (Ref. 54)	(^{7}Li,t) 15 MeV FRDWBA (Ref. 18)	Cluster model (Ref. 55)	Shell model (Ref. 56)
0.00, 0^+	1.00 (0.58)	1.00 (0.38)	1.00	1.00 (0.052)	1.00 (0.295)	1.00 (1.00)
1.63, 2^+	0.81	1.00	0.3	1.23	1.00	1.00
4.25, 4^+	0.36	0.75	0.2	1.25	0.95	1.00

duct of the α spectroscopic factors in the two nuclei. From the results of α-capture experiments on tritium, it has been determined[53] that the "cluster" reduced width for an $\alpha+t$ structure in ^{7}Li is about 20 times that for a single-particle configuration (^{6}Li$+n$ or ^{6}He$+p$) giving a value $S_\alpha(^7\text{Li}) = 0.95$. We have used this value in deriving the ^{20}Ne spectroscopic strengths listed in Table II. For the CCBA analysis it is not possible to perform a separate normalization for each state *a posteriori*, since the calculation includes interference terms between the various reaction amplitudes. In the present case, an initial choice of equal amplitudes for each of the 0^+, 2^+, and 4^+ transitions overestimated the 4^+ cross sections relative to the other two. A second iteration with the 4^+ transition amplitude reduced to 0.87 ($S_\alpha = 0.75$) resulted in the curves shown in Fig. 12. (Because of the contribution of the 4^+ transition to the 0^+ and 2^+ cross sections, this second calculation changed not only the relative magnitude of the 4^+ cross section but also the absolute magnitudes of all the cross sections.)

Table II also lists the relative values of S_α derived[54] from an analysis of the ^{16}O(^{6}Li, d)^{20}Ne reaction using the finite-range code LOLA. Kubo *et al.*[18] have carried out a finite-range DWBA analysis of ^{16}O(^{7}Li, t)^{20}Ne data taken at $E_{\text{Li}} = 15$ MeV using cluster wave functions calculated using the generator coordinate method. The extracted spectroscopic factors for their analysis are listed in Table II under the assumption that $S_\alpha(^7\text{Li}) = 0.95$. For comparison, the theoretical values for S_α (^{20}Ne) derived from model calculations by Matsuse and Kamimura[55] and Draayer[56] are also shown. Very good agreement is seen between the results of the present CCBA analysis and the cluster model predictions,[55] both in terms of relative and absolute spectroscopic factors.

B. ^{20}Ne $K^\pi = 0^-$ band

Horiuchi and Ikeda have proposed[9] that the $K^\pi = 0^+$ (g.s.) and the $K^\pi = 0^-$ bands in ^{20}Ne are "twins," in that they have the same intrinsic structure and would form a single $K = 0$ band of an asymmetric rotor, except for the energy gap resulting from the possibility of the α-particle tunneling through the ^{16}O core. Calculations by Matsuse and Kamimura[55] suggest that the α-clustering should be *more* pronounced in the 0^- band than in the 0^+ ground-state band, and the dominance of the members of this band in the ^{16}O(^{7}Li, t)^{20}Ne spectrum (Fig. 3) seems to support this suggestion.

The results of the FRDWBA calculations for the first three members of this band are shown in Fig. 14. The extraction of α-particle spectroscopic factors for these states is complicated by

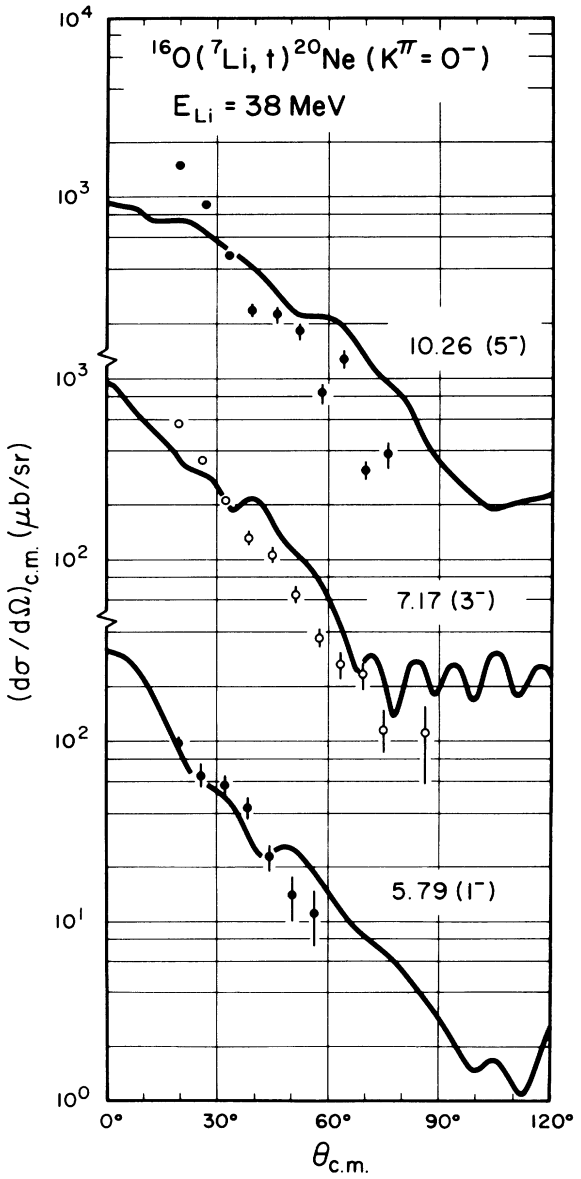

FIG. 14. Exact-finite-range DWBA analysis of the ^{16}O(^{7}Li,t)^{20}Ne ($K^\pi = 0^-$) data. The significance of the normalization of the curves is discussed in the text.

the fact that they are unbound. In the present case the wave functions for these states were normalized[28] by matching them to an asymptotic Coulomb wave function of the proper energy and then setting the integral of the wave function inside the matching radius ($R = 7.5$ fm) equal to unity. With this normalization, spectroscopic factors of 0.30 and 0.15 are extracted for the 1^- and 3^- states, respectively. In view of the uncertainties inherent in the normalization of the wave functions for these unbound states, the latter value is not inconsistent with the value of 0.36 extracted from ^{16}O(α, α)^{16}O elastic scattering[57]

for the 7.17 (3^-) state. The poor fit to the 5^- angular distribution probably results from the fact that this state is unbound by ≈ 5.5 MeV so that the use of a matching radius of 7.5 fm is inadequate. [The 5.79-MeV (1^-) and 7.17-MeV (3^-) states are unbound by only 1.06 and 2.4 MeV, respectively.]

C. ^{16}O $K^\pi = 0^+$ band

^{12}C(^{7}Li, t)^{16}O transitions to the members of the $K^\pi = 0^+$ 4p-4h band can proceed via a simple, one-step direct transfer and via a two-step process involving a four-nucleon transfer to one member of the band followed by inelastic excitation or deexcitation to another member of the band. Transitions to this band involving excitation of the ^{12}C (4.44-MeV, 2^+) state would have to be at least three-step, including core excitation in the entrance channel, four-nucleon transfer, and core deexcitation in the exit channel. In view of the weakness of two-step processes through the ^{12}C (4.44-MeV, 2^+) state for the ^{12}C(^{7}Li, t)^{16}O reaction, as indicated by the relatively weak noncompound-nuclear contributions to the transitions to the 9.85-MeV (2^+) and 11.10-MeV (4^+) states, this route was not included in our coupled-channels calculation for the ^{16}O $K^\pi = 0^+$ 4p-4h band. The calculation included only direct one-step transfers to the band and transfers to the band followed by inelastic excitations and deexcitations within the band, including the levels at 6.05 (0^+), 6.92 (2^+), and 10.35 (4^+) MeV. The FRDWBA and CCBA calculations for the 6.92-MeV (2^+) and 10.35-MeV (4^+) levels are shown in Fig. 15. From the FRDWBA analysis a spectroscopic factor of $S_\alpha = 1.10$ is extracted for the 6.92-MeV level. Since the 10.35-MeV level is unbound, its wave function was normalized using the same procedure[28] described above for the ^{20}Ne $K^\pi = 0^-$ band. The resulting spectroscopic factor $S_\alpha = 1.8$ is nearly seven times larger than the value of 0.27 obtained for this level from the analysis of ^{12}C(α, α)^{12}C elastic scattering.[58] For unbound states in the present analysis, the extraction of S_α is not very sensitive to the box-normalization radius for the final-state wave function; *however*, the evaluation of the transfer integral is very dependent on the extrapolation used for that wave function and on the choice of cutoff radius (10 fm in the present analysis). The CCBA analysis in Fig. 15 ($\beta_2 = 0.43$ and $\beta_4 = 0.25$) results in only very minor adjustments of S_α [$S_\alpha(2^+) = 1.0$ and $S_\alpha(4^+) = 1.8$], indicative of the very strong, direct, one-step component for this transition.

D. ^{16}O* (7.12-MeV, 1^-) state

In view of the astrophysical significance of the 7.12-MeV (1^-) excited state in ^{16}O as a subthreshold (B.E. = 42 keV) resonance for the ^{12}C(α, γ)^{16}O reaction,[59] we carried out an FRDWBA analysis of our measured angular distribution for this state. Using a 60% (1p-1h) + 40% (3p-3h) wave function for this state,[48] the resulting fit (see Fig. 16) determines a spectroscopic factor $S_\alpha = 0.20$, which is consistent with the value $\theta_\alpha^2(7.12)/\theta_\alpha^2(9.60) = 0.19$ obtained from an analysis[11] of the (α, γ) data. However, in view of the importance of compound-nuclear contributions to the measured (^{7}Li, t) cross sections for this state {the calculated $(d\sigma/d\Omega)_{HF}$ for this state [normalized to the 8.88-MeV (2^-) state] is approximately half the measured cross section at forward angles}, our extracted value should be considered uncertain by at least a factor of 2.

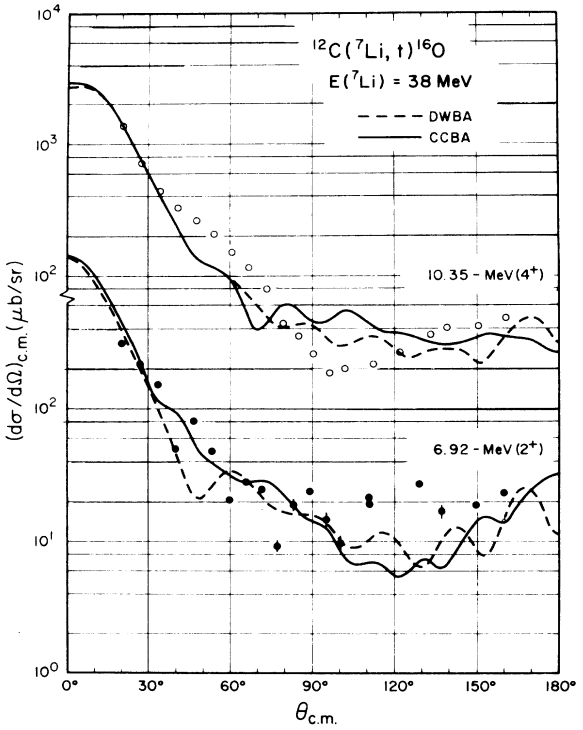

FIG. 15. Exact-finite-range DWBA and CCBA analyses of the ^{12}C(^{7}Li,t)^{16}O angular distributions for the 6.92-MeV (2^+) and 10.35-MeV (4^+) members of the 4p-4h $K^\pi = 0^+$ band. The significance of the normalization of the curves is discussed in the text.

VII. CONCLUSIONS

This work has been carried out to investigate the importance of FRCCBA and compound-nucleus contributions to these four-nucleon stripping reactions. Although this is not a definitive or complete analysis, in general there is reasonable agreement between the finite-range DWBA and Hauser-Feshbach calculations described above and these (^{7}Li, t) data, and α-cluster spectro-

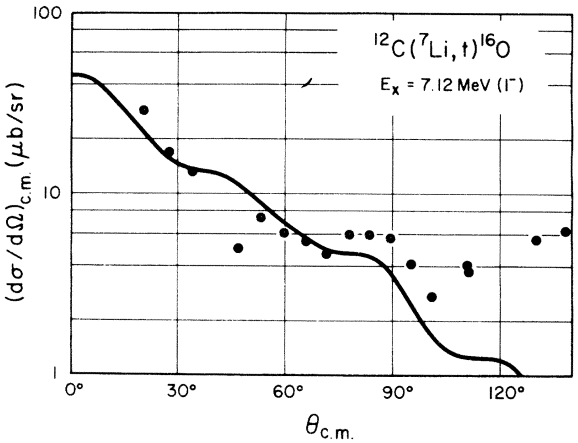

FIG. 16. Exact-finite-range DWBA analysis of the $^{12}C(^7Li,t)^{16}O$ transition to the 7.12-MeV (1^-) state, assuming a wave function for this state which is 60% (1p-1h) and 40% (3p-3h). The significance of the normalization of the curve and the extracted spectroscopic factor is discussed in the text.

scopic factors have been extracted for the bound states in the residual ^{16}O and ^{20}Ne nuclei. In the CCBA analysis, inelastic processes have been shown to make important contributions to the (^7Li, t) transitions and to make significant changes in the absolute magnitude of the extracted spectroscopic factors S_α.

In the FRDWBA analysis the inclusion of recoil effects and the $l=1$ relative motion of the triton and α clusters in ^7Li allows several different L transfers to each transition (except 0^+ to 0^+), resulting in fairly featureless angular distributions with no striking L dependences. These results are in good agreement with the measured data, but unfortunately they do not allow the determination of J^π assignments from the simple measurements of angular distributions. As the next step in this program, experiments are currently underway using (^7Li, $t\alpha$) correlation measurements to study the decay properties of the α-cluster states which are so selectively populated at forward angles in the (^7Li, t) reaction. Experiments are also in progress to extend these (^7Li, t) measurements to higher bombarding energies, $E(^7Li) = 52$ to 56 MeV using the Yale HR-MP tandem, in order to investigate the selective population of cluster states at excitation energies of up to 30 MeV.

ACKNOWLEDGMENTS

It is a special pleasure to thank the physicists and staff of the Brookhaven National Laboratory tandem accelerator for their gracious hospitality and assistance during the performance of these experimental measurements and to thank Dr. Robert Ascuitto for his indispensable contributions to the coupled-channels analysis. We are also grateful to Dr. James Vary for providing us with his cluster wave functions before their publication and to Dr. David Hanson for his assistance with the Hauser-Feshbach calculations.

*Work supported in part by U.S. AEC contract AT(11-1)-3074.

†Present address: Tandem Accelerator Laboratory, University of Pennsylvania, Philadelphia, Pennsylvania 19174.

‡Present address: Brookhaven National Laboratory, Upton, Long Island, New York 11973.

[1]K. Bethge, Annu. Rev. Nucl. Sci. 20, 255 (1970).

[2]A. A. Ogloblin, in *Nuclear Reactions Induced by Heavy Ions*, edited by R. Bock and W. R. Hering (North-Holland, Amsterdam, 1970), p. 231; Fiz. Elem. Chast. Atom. Yad. 3, 936 (1972) [Sov. J. Part. Nucl. 3, 467 (1973)].

[3]R. Middleton, in *Nuclear Reactions Induced by Heavy Ions* (see Ref. 2), p. 263.

[4]K. Bethge, in *Nuclear Reactions Induced by Heavy Ions* (see Ref. 2), p. 277.

[5]A. Arima and S. Yoshida, Nucl. Phys. A219, 475 (1974).

[6]D. Kurath, Phys. Rev. C 7, 1390 (1973).

[7]A. Arima, V. Gillet, and J. N. Ginocchio, Phys. Rev. Lett. 25, 1043 (1970).

[8]K. Ikeda *et al.*, Prog. Theor. Phys. Suppl. 52, 1 (1972).

[9]H. Horiuchi and K. Ikeda, Prog. Theor. Phys. 40, 277 (1968).

[10]C. A. Barnes, Advan. Nucl. Phys. 4, 133 (1971).

[11]S. E. Koonin, T. A. Tombrello, and G. Fox, Nucl. Phys. A220, 221 (1974).

[12]G. Michaud and W. A. Fowler, Ap. J. 173, 157 (1972).

[13]R. G. Couch and K. C. Shane, Ap. J. 169, 413 (1971).

[14]K. Meier-Ewert, K. Bethge, and K. O. Pfeiffer, Nucl. Phys. A110, 142 (1968).

[15]R. E. Segel, P. T. Debevec, and H. T. Fortune, Bull. Am. Phys. Soc. 18, 550 (1973); P. T. Debevec, H. T. Fortune, R. E. Segel, and J. F. Tonn, Phys. Rev. C 9, 2451 (1974).

[16]P. Neogy, W. Scholz, J. Garrett, and R. Middleton, Phys. Rev. C 2, 2149 (1970).

[17]F. Pühlhofer, H. G. Ritter, R. Bock, G. Brommundt, H. Schmidt, and K. Bethge, Nucl. Phys. A147, 258 (1970).

[18]K. I. Kubo and M. Hirata, Nucl. Phys. A187, 186 (1972); K. I. Kubo, *ibid.* A187, 205 (1972); K. I. Kubo, F. Nemoto, and H. Bando, *ibid.* A224, 573 (1974).

[19]N. Austern, R. M. Drisko, E. C. Halbert, and G. R. Satchler, Phys. Rev. 133, B3 (1964).

[20]R. M. DeVries, Phys. Rev. C 8, 951 (1973); 11, 2105 (1975).

[21]D. J. Pisano, Phys. Rev. C 14, 468 (1976) (second preceding paper, Paper I).

[22]R. J. Ascuitto and N. K. Glendenning, Phys. Rev. 181, 1396 (1969).

[23]R. Middleton, C. T. Adams, and K. Bethge, Nucl. Instrum. Methods 61, 115 (1968).
[24]V. Radeka, Brookhaven National Laboratory Report No. BNL 7448 (unpublished).
[25]K. P. Artemov, V. Z. Goldberg, I. P. Petrov, V. P. Rudakov, I. N. Serikov, and V. A. Timofeev, Phys. Lett. 37B, 61 (1971).
[26]T. K. Alexander, in *Proceedings of the Fifth Symposium on the Structure of Low-Medium Mass Nuclei, Lexington, Kentucky*, edited by J. P. Davidson and B. D. Kern (U.P. of Kentucky, Lexington, 1973), p. 272.
[27]O. Hausser, T. K. Alexander, D. L. Disdier, A. J. Ferguson, A. B. McDonald, and I. S. Towner, Nucl. Phys. A216, 617 (1973).
[28]J. P. Vary and C. B. Dover, Phys. Rev. Lett. 31, 1910 (1973); B. Buck, C. B. Dover, and J. P. Vary, Phys. Rev. C 11, 1803 (1975); J. P. Vary (private communication).
[29]For a discussion of the arguments surrounding this state, see R. Middleton, in Proceedings of the Heavy Ion Summer Study, Oak Ridge National Laboratory, 2 June–1 July 1972, edited by S. F. Thornton (unpublished), CONF-720669, p. 315; H. T. Fortune, R. R. Betts, and R. Middleton, Phys. Rev. C 10, 2135 (1974).
[30]M. E. Cobern and P. D. Parker (unpublished).
[31]D. Branford, N. Gardner, and I. F. Wright, Phys. Lett. 36B, 456 (1971).
[32]e.g., D. A. Bromley *et al.*, J. Phys. (Paris) 32, C6-5 (1971).
[33]M. Lepareux, N. Saunier, C. Gerardin, M. Wery, A. Foti, G. Pappalardo, and A. Strazzeri, Lett. Nuovo Cimento 8, 725 (1973).
[34]K. Bethge, K. Meier-Ewert, K. Pfeiffer, and R. Bock, Phys. Lett. 24B, 663 (1967).
[35]F. G. Perey, Phys. Rev. 131, 745 (1963).
[36]G. Bassani, N. Saunier, B. M. Traore, J. Raynal, A. Foti, and G. Pappalardo, Nucl. Phys. A189, 353 (1972).
[37]K. Bethge, C. M. Fou, and R. W. Zurmühle, Nucl. Phys. A123, 521 (1969).
[38]K. A. Weber, K. Meier-Ewert, H. Schmidt-Bocking, and K. Bethge, Nucl. Phys. A186, 145 (1972).
[39]P. Schumacher, N. Ueta, H. H. Duhm, K. I. Kubo, and W. J. Klages, Nucl. Phys. A212, 573 (1973).
[40]R. G. Stokstad, Yale University Wright Nuclear Structure Laboratory Internal Report No. 52 (unpublished).
[41]D. L. Hanson, R. G. Stokstad, K. A. Erb, C. Olmer, and D. A. Bromley, Phys. Rev. C 9, 929 (1974).
[42]U. Facchini and E. Saetta-Menichella, Energ. Nucl. (Milan) 15, 54 (1968).
[43]C. M. Perey and F. G. Perey, Nucl. Data A10, 539 (1972).
[44]J. D. Garrett and O. Hansen, Nucl. Phys. A212, 600 (1973).
[45]M. E. Cobern, Ph.D. thesis, Yale University, 1974 (unpublished).
[46]F. Ajzenberg-Selove, Nucl. Phys. A166, 1 (1971).
[47]J. Lowe and A. R. Barnett, Nucl. Phys. A187, 323 (1972).
[48]A. P. Zucker, B. Buck, and J. B. McGrory, Phys. Rev. Lett. 21, 39 (1968).
[49]C. A. Engelbrecht and H. A. Weidenmüller, Phys. Rev. C 8, 859 (1973).
[50]N. K. Glendenning, in *Proceedings of the International School of Physics "Enrico Fermi," Course XL*, edited by M. Jean (Academic, New York, 1969), p. 332.
[51]R. deSwiniarski, C. Glashausser, D. L. Hendrie, J. Sherman, A. D. Bacher, and E. A. McClatchie, Phys. Rev. Lett. 23, 317 (1969).
[52]R. J. Ascuitto, C. H. King, L. J. McVay, and B. Sorensen, Nucl. Phys. A226, 454 (1974).
[53]T. A. Tombrello and G. C. Phillips, Phys. Rev. 122, 224 (1961); T. A. Tombrello and P. D. Parker, *ibid.* 131, 2582 (1963).
[54]H. E. Gove, Bull. Am. Phys. Soc. 19, 1005 (1974).
[55]T. Matsuse and M. Kamimura, Prog. Theor. Phys. 49, 1765 (1973).
[56]J. P. Draayer, Nucl. Phys. A237, 157 (1975).
[57]F. Ajzenberg-Selove, Nucl. Phys. A190, 1 (1972).
[58]C. M. Jones, G. C. Phillips, R. W. Harris, and E. H. Beckner, Nucl. Phys. 37, 1 (1962).
[59]e.g., P. Dyer and C. A. Barnes, Nucl. Phys. A233, 495 (1974).